Journal of Solid State Chemistry 183 (2010) 2963–2967

Contents lists available at ScienceDirect

Journal of Solid State Chemistry

journal homepage: www.elsevier.com/locate/jssc

Crystal structure and magnetic properties of $Ce_7Ni_{5\pm x}Ge_{3\pm x}In_6$ and $Pr_7Ni_{5\pm x}Ge_{3\pm x}In_6$

Nataliya Chumalo [a,b], Galyna P. Nychyporuk [a], Volodymyr V. Pavlyuk [a], Rainer Pöttgen [b,*], Dariusz Kaczorowski [c], Vasyl' I. Zaremba [a]

[a] Department of Inorganic Chemistry, Ivan Franko National University of Lviv, Kyryla i Mefodiya 6, 79005 Lviv, Ukraine
[b] Institut für Anorganische und Analytische Chemie, Universität Münster, Corrensstraße 30, D-48149 Münster, Germany
[c] Institute of Low Temperature and Structure Research, Polish Academy of Sciences, P.O. Box 1410, 50-950 Wroclaw, Poland

ARTICLE INFO

Article history:
Received 27 July 2010
Received in revised form
28 September 2010
Accepted 3 October 2010
Available online 13 October 2010

Keywords:
Intermetallic compounds
Crystal chemistry
Magnetic properties

ABSTRACT

The indides $Ce_7Ni_{5\pm x}Ge_{3\pm x}In_6$ and $Pr_7Ni_{5\pm x}Ge_{3\pm x}In_6$ were synthesized from the elements by arc-melting of the components. Single crystals were grown via special annealing sequences. Both structures were solved from X-ray single crystal diffraction data: new structure type, $P6/m$, $Z=1$, $a=11.385(2)$, $c=4.212(1)$ Å, $wR_2=0.0640$, $634F^2$ values, 25 variables for $Ce_7Ni_{4.73}Ge_{3.27}In_6$ and $a=11.355(6)$, $c=4.183(2)$ Å, $wR_2=0.0539$, $563F^2$ values, 25 variables for $Pr_7Ni_{4.96}Ge_{3.04}In_6$. Both indides show homogeneity ranges through Ni/Ge mixing (M sites). This new structure type can be derived from the AlB_2 structure type by a substitution of the Al and B atoms by CeM_{12} and $NiIn_6Ce_3$ polyhedra (tricapped trigonal prism). Magnetic susceptibility measurements on a polycrystalline sample of $Ce_7Ni_5Ge_3In_6$ indicated Curie–Weiss like paramagnetic behavior down to 1.71 K with the effective magnetic moment slightly reduced in relation to the value expected for trivalent cerium ions. No magnetic ordering is evident.

1. Introduction

The ternary indides $RE_xT_yIn_z$ (RE=rare earth element, T=transition metal) show a large variety of bonding and coordination patterns: (i) complex rare earth metal-rich structures with high coordination numbers, (ii) transition metal clustering, (iii) the formation of three-dimensional $[T_yIn_z]$ polyanionic networks which leave cavities or channels for the rare earth elements, or (iv) distorted *bcc* indium cubes as substructures in indium-rich compounds. The structural chemistry of these materials has been summarized in a review article [1].

Within the large family of $RE_xT_yIn_z$ indides several simple compositions (although with different structure type) occur frequently with a large number of representatives. Besides more than the 90 equiatomic compounds *RET*In [1], the RE_2T_2In and RE_2Ge_2In indides (more than 80 representatives) [2] have intensively been studied, especially with respect to their physical properties. These indides crystallize in four different structure types, i.e. Mo_2B_2Fe, Mn_2B_2Al, Er_2Au_2Sn (U_2Pt_2Sn), and W_2B_2Co; the major part (more than 80%), however, adopts the tetragonal Mo_2B_2Fe type [3]. These compounds exhibit interesting physical properties and they have attracted the interest of solid state chemists and physicists for many years. To give some examples, Ce_2Pt_2In is classified as a heavy fermion system [4], and cerium is in a stable trivalent state in Ce_2Rh_2In and Ce_2Pd_2In [5]. An efficient way to influence the physical properties of such compounds is the substitution of one of the components in the solid solutions $RE_{2-x}RE'_xM_2In$ and $RE_2T_{2-x}T'_xIn$. Various examples of such solid solutions have been presented. For the series $Ce_2Pd_{2-x}Ni_xIn$ the magnetic properties change from ferromagnetic Ce_2Pd_2In (T_C=4 K) to temperature independent paramagnetic Ce_2Ni_2In, caused by substitution of Pd by Ni [6]. Substitution of paramagnetic Ce atoms by diamagnetic La, Y, or Lu in Ce_2Rh_2In and Ce_2Pd_2In [5] causes formation of the heavy fermion compounds $Y_{1.6}Ce_{0.4}Pd_2In$ and $Lu_{1.6}Ce_{0.4}Pd_2In$. An interesting structural feature of this family of compounds is the fact, that the transition metal site can be completely substituted by the main group element germanium [7,8]. Such a substitution has a drastic effect on the electronic situation of the rare earth element and thus on the magnetic properties. However, recent investigations of the possible quasi-ternary system $Ce_2Ni_{2-x}Ge_xIn$ (x=0–2) at 870 K clearly indicated that there is no solubility of Ge in Ce_2Ni_2In (and Ni in Ce_2Ge_2In).

Instead of a continuous solid solution $Ce_2Ni_{2-x}Ge_xIn$, our phase analytical investigations revealed the existence of a new quaternary germanide indide $Ce_7Ni_5Ge_3In_6$ with an unknown structure. The structure investigations of $Ce_7Ni_5Ge_3In_6$ and the isotypic praseodymium compound and the magnetic data of $Ce_7Ni_5Ge_3In_6$ are presented herein.

* Corresponding author. Fax: +49 251 83 36002.
E-mail address: pottgen@uni-muenster.de (R. Pöttgen).

0022-4596/$ - see front matter © 2010 Elsevier Inc. All rights reserved.
doi:10.1016/j.jssc.2010.10.005

2. Experimental

2.1. Synthesis

Starting materials for the preparation of the $RE_7Ni_5Ge_3In_6$ (RE=Ce, Pr) samples were ingots of the rare earth elements (Johnson Matthey), nickel wire (Johnson Matthey), germanium lumps (Wacker) and indium tear drops (Chempur), all with stated purities better than 99.9%. The initial composition of the compounds was determined during phase analysis of polished buttons of samples from the $Ce_2Ni_{2-x}Ge_xIn$ system by means of EDX analysis (LEICA 420i scanning electron microscope).

In a first step, the cerium and praseodymium ingots were cut into smaller pieces and arc-melted [9] to small buttons (about 500 mg) under 700 mbar pressure of argon gas. Titanium sponge was used as a getter material. Subsequently the melted cerium/or praseodymium buttons were mixed with pieces of nickel and germanium and indium tear drops in the ideal 7:5:3:6 atomic ratio and arc-melted under the same conditions. The product pellets were re-melted three times to ensure homogeneity. The total weight loss after the melting procedure was smaller than 0.5%. After the arc-melting procedure the $RE_7Ni_5Ge_3In_6$ (RE=Ce, Pr) indides were obtained only as polycrystalline powders.

Single crystals were grown using a special heat treatment. Parts of arc-melted samples (about 750 mg) were put in small tantalum containers that have been sealed in evacuated silica tubes as an oxidation protection. The ampoules were first heated to 1275 K (for both compounds) within 5 h and held at that temperature for another 5 h. Subsequently, the temperature was lowered at a rate of 5 K/h to 1000 K, then at a rate of 15 K/h to 700 K, and finally cooled to room temperature within 10 h. After cooling, the samples could easily be separated from the tantalum container. No reaction of the container material was evident. The brittle samples of both compounds are stable in air over weeks in powdered as well as in polycrystalline form. The irregularly shaped single crystals exhibit metallic luster.

2.2. Scanning electron microscopy

The single crystals investigated on the diffractometer were analyzed in a scanning electron microscope (LEICA 420i) through energy dispersive analysis of X-rays using CeO_2, PrF_3, Ni, Ge and InAs as standards. No impurity elements heavier than sodium were observed. The composition determined by EDX (35 ± 2 at% RE: 23 ± 2 at% Ni: 15 ± 2 at% Ge: 27 ± 2 at% In) is in good agreement with the ideal composition, i.e. 33.3:23.8:14.3:28.6. The standard uncertainties account for the analysis at various points on the crystal surfaces.

2.3. X-ray powder and single crystal data

The polycrystalline samples were studied through Guinier powder patterns (imaging plate technique, Fujifilm BAS–1800) using CuKα_1 radiation and α-quartz (a=4.9130 and c=5.4046 Å) as an internal standard. The lattice parameters were obtained from least-squares fits of the powder data. The correct indexing of the patterns was ensured through intensity calculations [10] taking the atomic positions from the structure refinements. The powder lattice parameters compared well with the single crystal data.

Irregularly shaped single crystals of both compounds were selected from the annealed sample by mechanical fragmentation. They were investigated by Laue photographs on a RKV-86 camera (white molybdenum radiation, photo technique) in order to check the quality for intensity data collection. Intensity data were measured at room temperature on an Oxford Diffraction Xcalibur automatic diffractometer with CCD detector (Mo$K\alpha$-radiation, graphite monochromator, ω-scan). The data collection and reduction were performed using the CrysAlis CCD [11] and CrysAlis Red [12] programs. All relevant crystallographic data and details of the data collections are listed in Table 1.

The structure of $Ce_7Ni_5Ge_3In_6$ was determined first. Careful analysis of the diffractometer data revealed a primitive trigonal or hexagonal unit cell and the observed systematic extinctions were compatible with space group $P\bar{3}$ (*translationengleiche* subgroup of $P6/m$) and $P6/m$, of which the centrosymmetric hexagonal $P6/m$ group was found to be correct during structure refinement. The starting atomic parameters were determined by an interpretation of direct methods with SHELXS-97 [13] and the structure was refined with anisotropic displacement parameters for all atoms with SHELXL-97 [14] (full matrix least squares on F_o^2). The occupancy parameters have been refined in a separate series of least squares cycles. Refinement of the occupancy parameters revealed a mixed Ni/Ge (called M) occupancy for the 6k site. This occupancy parameter was refined as least-squares variable in the final cycles, leading to the composition $Ce_7Ni_{4.73}Ge_{3.27}In_6$ for the investigated crystal, in good agreement with the EDX data. All other sites were fully occupied within two standard uncertainties. Final difference Fourier synthesis revealed no significant residual peaks. The structural model of the cerium compound was used as the initial model for the praseodymium one. The refinement readily converged to the residuals listed are in Table 1. The refined atomic parameters and interatomic distances are listed in Tables 2 and 3.

Further details on the structure refinements are available. Details may be obtained from: Fachinformationszentrum Karlsruhe, D-76344 Eggenstein-Leopoldshafen (Germany) by quoting Registry nos. CSD–421990 ($Ce_7Ni_{4.73}Ge_{3.27}In_6$) and CSD–421991 ($Pr_7Ni_{4.96}Ge_{3.04}In_6$).

2.4. Physical properties

Magnetic measurements were performed in the temperature range 1.7–300 K and in applied magnetic fields up to 5 T employing a Quantum Design MPMS-5 superconducting quantum interference device (SQUID) magnetometer. For these measurements small pellets of pressed polycrystalline powders were utilized which were placed in small gelatin capsules.

Table 1
Crystal data and structure refinement for $Ce_7Ni_{4.73}Ge_{3.27}In_6$ and $Pr_7Ni_{4.96}Ge_{3.04}In_6$, space group $P6/m$, Z=1.

Empirical formula	$Ce_7Ni_{4.73}Ge_{3.27}In_6$	$Pr_7Ni_{4.96}Ge_{3.04}In_6$
Molar mass	2184.83	2187.17
Unit cell dimensions	a=11.385(2) Å	a=11.355(6) Å
(powder data)	c=4.212(1) Å	c=4.183(2) Å
Calculated density	7.67 g/cm^3	7.78 g/cm^3
Absorption coefficient	33.3 mm^{-1}	34.7 mm^{-1}
F(0 0 0)	937	943
Crystal size	$15\times50\times80$ μm^3	$10\times25\times75$ μm^3
θ range for data collection	3–33°	3–31°
Range in hkl	±16, ±16, ±6	±16, ±16, $-6\le l\le2$
Total no. reflections	4381	4123
Independent reflections	634	563
Reflections with $I>2\sigma(I)$	571	501
Data/parameters	634/25	563/25
Goodness-of-fit on F^2	1.306	1.351
Final R indices [$I>2\sigma(I)$]	$R1$=0.0244	$R1$=0.0223
	wR_2=0.0554	wR_2=0.0502
R indices (all data)	$R1$=0.0307	$R1$=0.0281
	wR_2=0.0640	wR_2=0.0539
Extinction coefficient	0.0074(4)	0.0068(3)
Largest diff. peak and hole	3.13 and −2.49 e/Å^3	2.02 and −1.74 e/Å^3

Table 2
Atomic coordinates and anisotropic displacement parameters (pm^2)* for $Ce_7Ni_{4.73}Ge_{3.27}In_6$ and $Pr_7Ni_{4.96}Ge_{3.04}In_6$.

Atom	Wyckoff	x	y	z	U_{11}	U_{22}	U_{33}	U_{12}	U_{eq} [c] site
$Ce_7Ni_{4.73}Ge_{3.27}In_6$									
Ce1	1*a*	0	0	0	80(2)	U_{11}	107(4)	40(1)	88(2)
Ce2	6*j*	0.30278(4)	0.38070(4)	0	113(2)	81(2)	109(2)	41(1)	104(1)
In	6*k*	0.16667(5)	0.51751(5)	1/2	112(2)	90(2)	131(2)	49(2)	112(2)
Ni2	2*c*	1/3	2/3	0	151(5)	U_{11}	119(7)	76(2)	141(3)
M [a]	6*k*	0.23965(9)	0.15842(8)	1/2	143(5)	111(5)	137(5)	84(3)	121(3)
$Pr_7Ni_{4.96}Ge_{3.04}In_6$									
Pr1	1*a*	0	0	0	54(3)	U_{11}	102(4)	27(1)	70(2)
Pr2	6*j*	0.30177(4)	0.38061(4)	0	82(2)	54(2)	100(2)	27(1)	82(1)
In	6*k*	0.16522(5)	0.51720(5)	1/2	85(3)	65(3)	126(3)	37(2)	92(2)
Ni2	2*c*	1/3	2/3	0	115(5)	U_{11}	111(8)	61(4)	114(3)
M [b]	6*k*	0.23971(9)	0.15947(9)	1/2	102(5)	73(5)	132(6)	58(2)	95(4)

*$U_{13}=U_{23}=0$.

[a] $M=0.54(3)$ Ge+0.46(3) Ni.
[b] $M=0.51(4)$ Ge+0.49(4) Ni.
[c] U_{eq} is defined as one-third of the trace of the orthogonalized U_{ij} tensor.

Table 3
Interatomic distances (Å) in the structure of $Ce_7Ni_{4.73}Ge_{3.27}In_6$ and $Pr_7Ni_{4.96}Ge_{3.04}In_6$. Standard deviations are all equal or smaller than 0.001 Å.

			RE=Ce	*RE*=Pr
*RE*1:	12	*M*	3.196	3.183
	6	*RE*2	3.966	3.951
*RE*2:	2	*M*	3.054	3.039
	2	*M*	3.088	3.067
	1	Ni2	3.097	3.085
	2	In	3.370	3.356
	2	In	3.417	3.403
	2	In	3.422	3.404
	1	*RE*2	3.917	3.926
	3	*RE*2	3.966	3.951
In:	2	Ni2	2.774	2.768
	1	*M*	2.806	2.796
	2	In	3.128	3.139
	2	*RE*2	3.370	3.356
	2	*RE*2	3.417	3.403
	2	*RE*2	3.422	3.404
	1	In	3.613	3.573
Ni2:	6	In	2.774	2.768
	3	*RE*2	3.097	3.085
M:	2	*M*	2.403	2.400
	1	In	2.806	2.796
	2	*RE*2	3.054	3.039
	2	*RE*2	3.088	3.067
	2	*RE*1	3.196	3.183

3. Result and discussion

3.1. Crystal chemistry

$Ce_7Ni_{4.73}Ge_{3.27}In_6$ and $Pr_7Ni_{4.96}Ge_{3.04}In_6$ crystallize with a new structure type. As an example we present a projection of the $Ce_7Ni_{4.73}Ge_{3.27}In_6$ structure in Fig. 1. From a geometrical point of view, the $Ce_7Ni_{4.73}Ge_{3.27}In_6$ structure can be derived from the well known AlB_2 type, which is known for the solid solutions $Ce(Ni_{1-x}In_x)_2$ [15] and $Ce(Ni_{1-x}Ge_x)_2$ [16,17]. An ordered substitution of the aluminum sites by $[CeM_{12}]$ hexagonal prisms and of the boron sites by tricapped trigonal prisms $[NiIn_6Ge_3]$ (Fig. 2) leads to the structure of $Ce_7Ni_{4.73}Ge_{3.27}In_6$ (in the following denoted as $Ce_7Ni_5Ge_3In_6$) according to $[Ce(Ni_{0.5}Ge_{0.5})_6]+2[NiIn_3Ge_3]=Ce_7Ni_5Ge_3In_6$. The packing pattern of the polyhedra in $Ce_7Ni_5Ge_3In_6$ is shown in Fig. 3.

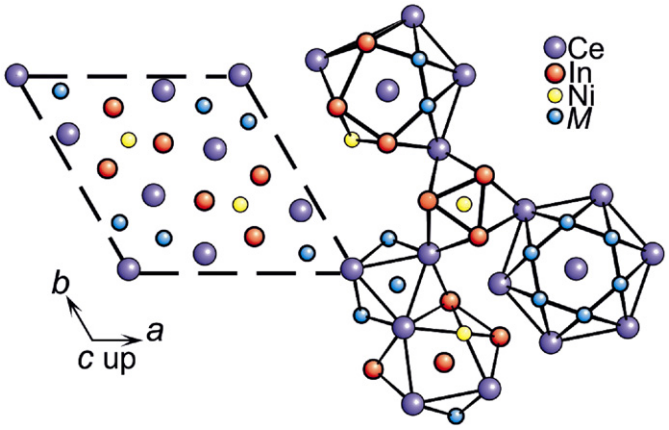

Fig. 1. Projection of the $Ce_7Ni_5Ge_3In_6$ structure along the *c* axis. All atoms lie on mirror planes at $z=0$ (thin lines) and $z=1/2$ (thick lines).

First we need to comment on the mixed occupied sites 6*k* with refined occupancy values of $M=0.54(3)$ Ge+0.46(3) Ni and $M=0.51(4)$ Ge+0.49(4) Ni for the cerium and praseodymium compound, respectively. In view of the standard uncertainties, we observe an almost 50/50 occupancy which hints for an ordering of the nickel and germanium atoms. Such an ordering would be possible upon splitting the 6*k* site into 2 three-fold sites. We have refined both structures also in space group $P\bar{6}$ (*translationengleiche* subgroup of $P6/m$) with two 3*k* sites. However, these refinements still did not resolve the mixed occupancies and we therefore kept the centrosymmetric space group. Ordered, but strongly puckered Ni_3Ge_3 hexagons occur in the structure of CeNiGe [18] with TiNiSi type structure. In $Ce_7Ni_5Ge_3In_6$ the mixed-occupied *M* site shows no pronounced U_{33} values which might indicate a puckering. Summing up, from the diffraction experiments we observe no long-range ordering of the nickel and germanium atoms within the M_6 hexagons, however, we expect, based on the largely different chemical potential of nickel and germanium, a high degree of short-range ordering. In extension of the single crystal work we investigated the homogeneity range for the cerium compound in more detail, leading to the solid solution in the small range $Ce_7Ni_{4.75-5.25}Ge_{3.25-2.75}In_6$. As emphasized in Fig. 4, further increase and decrease of the nickel content leads to biphasic samples. The side-products which were detected by powder X-ray diffraction are $RENi_{2-x}In_x$ with AlB_2 type and *RE*NiGe with TiNiSi type structure.

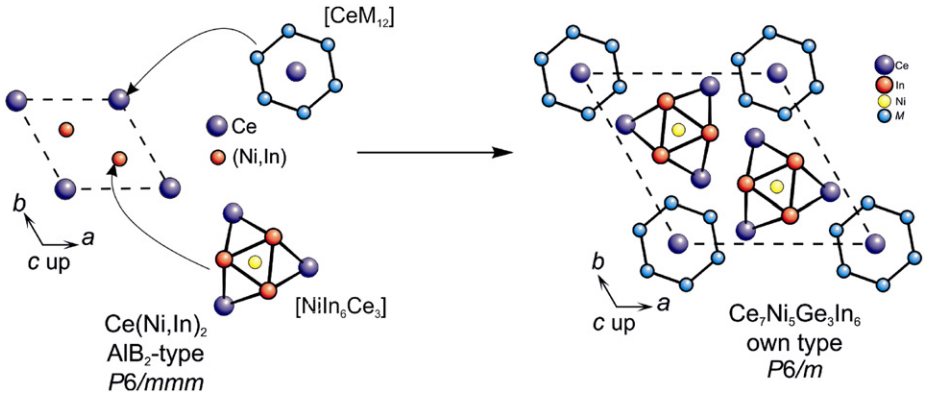

Fig. 2. Comparison of the $Ce_7Ni_5Ge_3In_6$ structure with the AlB_2 type *via* substitution of the aluminum and boron atoms by different building units. For details see text.

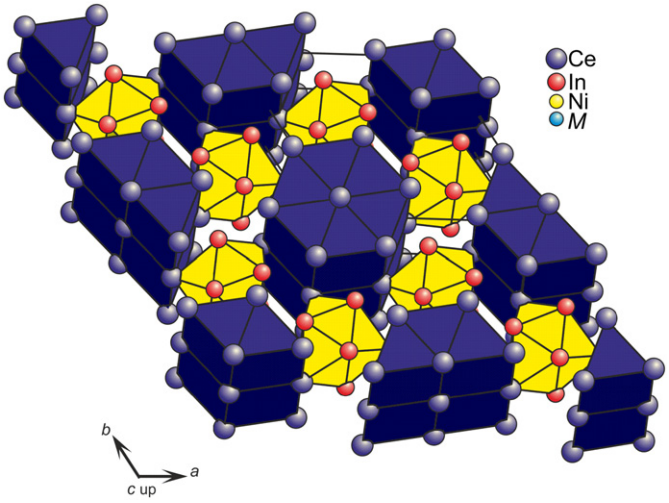

Fig. 3. Packing of the polyhedra in the $Ce_7Ni_5Ge_3In_6$ structure.

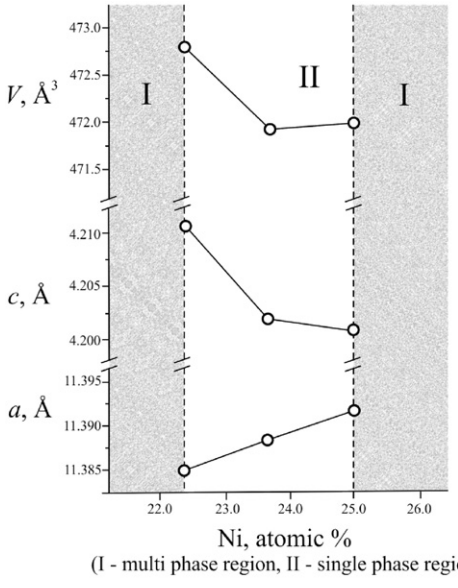

Fig. 4. Change of unit cell parameters (powder data) in the solid solution $Ce_7Ni_{4.75-5.25}Ge_{3.25-2.75}In_6$.

Within the M_6 hexagons the *M*–*M* distance of 240 pm is close to the sum of the covalent radii [19] for nickel and germanium of 237 pm. Similar Ni–Ge distances occur in the $NiGe_{4/4}$ tetrahedra in

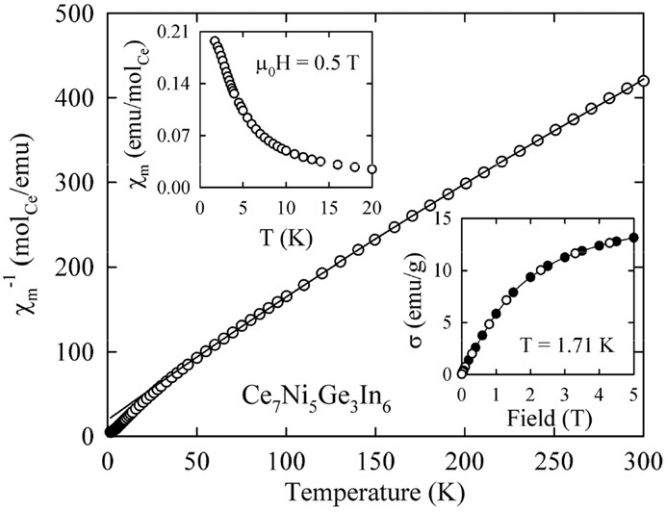

Fig. 5. Temperature dependence of the inverse molar magnetic susceptibility of $Ce_7Ni_5Ge_3In_6$. The solid line represents the Curie–Weiss fit discussed in the text. The upper inset displays the molar magnetic susceptibility at low temperatures measured in a field of 0.5 T. The lower inset shows the field variation of the magnetization taken at 1.71 K with increasing (full symbols) and decreasing (open symbols) magnetic field.

$NdNi_2Ge_2$ (237 pm) [20], also within the $NiGe_5$ pyramids of $CeNiGe_2$ (233–242 pm) [21] and within the planar Ni_3Ge_3 hexagons of the quaternary hydride $CeNiGeH_{1.6}$ [22]. We can thus assume substantial Ni–Ge bonding within the M_6 hexagons.

The nickel atoms within the tricapped trigonal prisms have six indium neighbors at Ni–In distances of 277 pm, slightly longer than the sum of the covalent radii [19] of 265 pm. This is also the typical coordination of part of the nickel atoms in ZrNiAl type CeNiIn [23] as well as for the Ni3 atoms (278–287 pm Ni–In) in $PrNiIn_2$ type $CeNiIn_2$ [24]. The indium atoms, building the triangular faces of the trigonal prisms have comparatively short In–In distances of 313 pm, shorter than in the tetragonal body-centered structure of elemental indium (a=325.2, c=494.7 pm) [25], where each indium atom has four nearest neighbors at 325 pm and eight further neighbors at 338 pm. These $NiIn_6$ trigonal prisms are capped by three cerium atoms on the rectangular faces at Ni2–Ce distances of 310 pm. The crystal chemical features of $Ce_7Ni_{5-}Ge_3In_6$ are similar to those of the many other $RE_xNi_yIn_z$ indides. For further details we refer to a review article [1].

3.2. Physical properties

The magnetic data obtained for a polycrystalline sample of $Ce_7Ni_5Ge_3In_6$ are summarized in Fig. 5. Above about 50 K the

inverse molar magnetic susceptibility can be described by a modified Curie–Weiss (MCW) law, $\chi=\chi_0+C/(T-\theta_p)$, with the temperature-independent contribution χ_0 equal to $3.0(1)\times10^{-4}$ emu/(mole Ce-atom), the paramagnetic Curie temperature $\theta_p=-12.6(2)$ K and the effective magnetic moment $\mu_{eff}=(8C)^{1/2}=2.28\ \mu_B$ per Ce atom. The term χ_0 representing a sum of Van Vleck paramagnetism, conduction-electrons paramagnetism and core-electrons diamagnetism is of the order usually found for cerium intermetallics containing *d*-electron transition elements. The experimental value of μ_{eff} is somewhat reduced in comparison to that expected within the Russell–Saunders coupling scheme for a stable trivalent cerium ion ($2.54\ \mu_B$). This feature may reflect some delocalization of cerium 4*f* electrons, possibly because of considerable hybridization between these electrons and the *s*, *p* and/or *d* electrons of the ligands. In line with such hypothesis seems the relatively large negative value of θ_p that hints at antiferromagnetic correlations, but possibly also at Kondo screening effect with the characteristic energy scale of about 3 K [26]. The latter scenario is further supported by the lack of any magnetic ordering down to 1.71 K, the terminal temperature in this study. As shown in the upper inset to Fig. 5, the magnetic susceptibility is featureless at low temperatures. The deviation of the $\chi^{-1}(T)$ curve from the MCW formula observed in this temperature region presumably arises from crystalline electric field interactions. The nonmagnetic ground state in this compound is corroborated by the behavior of the magnetization isotherm taken at 1.71 K (see the lower inset to Fig. 5). Apparently, the character of $\sigma(H)$ is typical of paramagnetic systems.

Acknowledgments

This work was financially supported by the Deutsche Forschungsgemeinschaft. N. C. indebted to the DAAD for a research stipend.

References

[1] Ya.M. Kalychak, V.I. Zaremba, R. Pöttgen, M. Lukachuk, R.-D. Hoffmann, Rare earth-transition metal-indides, in: K.A. Gschneidner Jr., V.K. Pecharsky, J.-C. Bünzli (Eds.), Handbook on the Physics and Chemistry of Rare Earths, vol. 34, Elsevier, Amsterdam2005, pp. 1–133 (Chapter 218).
[2] M. Lukachuk, R. Pöttgen, Z. Kristallogr. 218 (2003) 767.
[3] W. Rieger, H. Nowotny, F. Benesovsky, Monatsh. Chem. 95 (1964) 1502.
[4] R. Hauser, H. Michor, E. Bauer, G. Hilscher, D. Kaczorowski, Physica B 230 – 232 (1997) 211.
[5] R. Mallik, E.V. Sampathkumaran, J. Dumschat, G. Wortmann, Solid State Commun. 102 (1997) 59.
[6] Y. Ijiri, F.J. DiSalvo, J. Alloys Compd. 233 (1996) 69.
[7] V.I. Zaremba, J. Stepien'-Damm, G.P. Nychyporuk, Yu.B. Tyvanchuk, Ya.M. Kalychak, Crystallogr. Rep. 43 (1998) 8.
[8] V.I. Zaremba, D. Kaczorowski, G.P. Nychyporuk, U.Ch. Rodewald, R. Pöttgen, Solid State Sci. 6 (2004) 1301.
[9] R. Pöttgen, Th. Gulden, A. Simon, GIT Labor-Fachzeitschrift 43 (1999) 133.
[10] K. Yvon, W. Jeitschko, E. Parthé, J. Appl. Crystallogr. 10 (1977) 73.
[11] Oxford Diffraction, CrysAlis CCD, Version 1.170, Oxford Diffraction Ltd., Abingdon, Oxford, England, 2003.
[12] Oxford Diffraction, CrysAlis Red. Version 1.171, Oxford Diffraction Ltd., Abingdon, Oxford, England, 2005.
[13] G.M. Sheldrick, SHELXS-97 and SHELXL-97—WinGX Version, Release 97-2, University of Göttingen, Germany, 1997.
[14] G.M. Sheldrick, Acta Crystallogr. A64 (2008) 112.
[15] V.M. Baranyak, O.V. Dmytrakh, Ya.M. Kalychak, P.Yu. Zavalij, Inorg. Mater. 24 (1988) 873.
[16] E.I. Gladyshevskii, O.I. Bodak, Dopov. Akad. Nauk Ukr. RSR (1965) 601.
[17] P. Salamakha, M. Konyk, O. Sologub, O. Bodak, J. Alloys Compd 236 (1996) 206.
[18] J.P. Kuang, H.J. Cui, J.Y. Li, F.M. Yang, H. Nakotte, E. Brück, F.R. De Boer, J. Magn. Magn. Mater. 104–107 (1992) 1475.
[19] J. Emsley, The Elements, Oxford University Press, Oxford, 1999.
[20] G. Venturini, B. Malaman, J. Alloys Compd 235 (1996) 201.
[21] P. Schobinger-Papamantellos, A. Krimmel, A. Grauel, K.H.J. Buschow, J. Magn. Magn. Mater. 125 (1993) 151.
[22] F. Weill, M. Pasturel, J.-L. Bobet, B. Chevalier, J. Phys. Chem. Solids 67 (2006) 1111.
[23] R. Ferro, R. Marazza, G. Rambaldi, Z. Metallkd. 65 (1974) 37.
[24] V.I. Zaremba, Ya.M. Kalychak, Yu.B. Tyvanchuk, R.-D. Hoffmann, M.H. Möller, R. Pöttgen, Z. Naturforsch. 57b (2002) 791.
[25] J. Donohue, The Structures of the Elements, Wiley, New York, U.S.A, 1974.
[26] A.C. Hewson, The Kondo Problem to Heavy Fermions, Cambridge University Press, Cambridge, England, 1993.